https://doi.org/10.2352/ISSN.2470-1173.2021.16.COLOR-252
© 2021, Society for Imaging Science and Technology

# Improved Content-Color-Dependent Screening (CCDS): Adaptive Bilateral Filtering and Color-Aware Sobel Edge Detector[1]

*Yang Yan, Jan P. Allebach; Purdue University; West Lafayette, Indiana, United States*

## Abstract

*In previous work [1] , content-color-dependent screening (CCDS) determines the best screen assignments for either regular or irregular haltones to each image segment, which minimizes the perceived error compared to the continuous-tone digital image. The model first detects smooth areas of the image and applies a spatiochromatic HVS-based model for the superposition of the four halftones to find the best screen assignment for these smooth areas. The segmentation is not limited to separating foreground and background. Any significant color regions need to be segmented. Hence, the segmentation method becomes crucial. In this paper, we propose a general segmentation method with a few improvements: The number of K-means clusters is determined by the elbow method to avoid assigning the number of clusters manually for each image. The noise removing bilateral filter is adaptive to each image, so the parameters do not need to be tested and adjusted based on the visual output results. Also, some color regions can be clearly separated out from other color regions by applying a color-aware Sobel edge detector.*

## Introduction

Halftoning is a process to simulate a continuous-tone image with the use of various dots, either varying in size with the same spacing (amplitude modulation) or varying in spacing with the same size (frequency modulation) [2]. From this perspective, the types of haltone textures fall in either periodic or aperiodic and either clustered-dot or dispersed-dot. This is a continuing work based on periodic, clustered-dot halftones [3], which are more stable for electrophotographic printing.

To produce color prints, most laser, electrophotographic printers independently halftone four continuous-tone color separations, corresponding to four different colorants CMYK (cyan, magenta, yellow, and black), independently with screens rotated to some angles. The superposition of two or more lattices of screens may cause moire and/or rosette artifacts. To minimize these artifacts, the angles between the screens are fixed to 75°, 15°, 0°, and 45° for the four colorants respectively [3] [4]. However, these screens with specific angles still need to be assigned to each individual colorant. As stated in Jumabayeva's work [1], in order to improve the print quality, the best screen assignments are fixed by minimizing the perceived error compared to the continuous-tone original image.

For different colors, the best screen assignment selections usually are different as illustrated in Fig. 1. So, the image will be clustered and segmented into segments first, and then the best screen assignments will be decided for each segment based on the corresponding average color absorptance value contained within that segment. In this case, the image is not only segmented into foreground and background but also into any reasonable set of color regions. Each region contains pixels with similar colors.

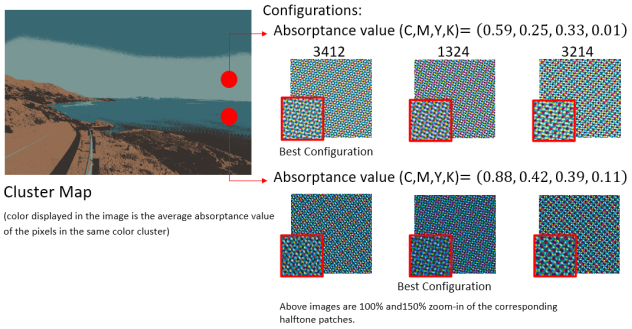


***Figure 1.*** *For different colors, the best screen assignment selections are different. The 4-digit configuration numbers ("3412", "1342", and "3214") are the screen indices of a screen set assigned to cyan, magenta, yellow and black channels.*

This paper mainly focuses on improving the clustering and segmentation approaches in a general implementation for efficiently generating the halftone results for various images. The following section is divided into several sub-sections to highlight these improvements.

The idea of segmenting the image and rendering the halftone results by regions has also been investigated by others. Liu et al. [15] segmented the image into regions according to the frequencies. They employed inter-iterative clustered-dot direct multi-bit search (CLU-DMS) [15] to generate high quality screens of different spatial frequencies and applied them to the image regions of different frequencies. This method employed multiple sets of screens but was not applied to color images.

## Methods

The previous method [1] provides a nice overall structure for the processes from the digital continuous-tone image to the haltone screened image.

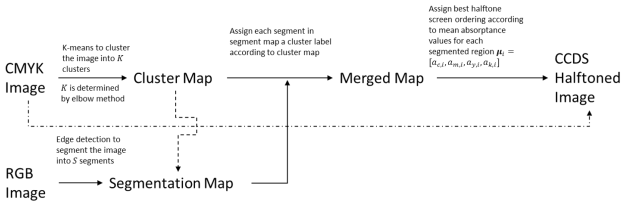


***Figure 2.*** *Overall structure of the CCDS algorithm.*

The new algorithm is based on a similar overall structure. The updated structure is shown as a flow chart in Fig. 2, which

[1]Research supported by HP Indigo Division, Rehovat, ISRAEL.

consists of four main parts. These four main parts include generating the cluster map using the elbow method with the K-means algorithm [7], generating the segmentation map with adaptive bilateral filtering [5] and the color-aware Sobel edge detector, merging the cluster map and segmentation map to generate the merged map, and the final procedure: rendering the halftoned image with the best screen assignment for each cluster.

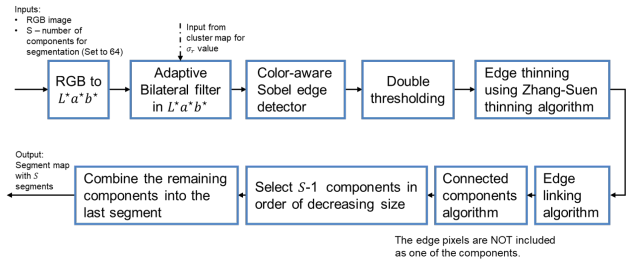


***Figure 3.*** *Segmentation Algorithm.*

The updated detailed flow chart for generating the segmentation map is shown in Fig. 3 [5] [11] [12] [13]. Other than updates to the bilateral filtering and edge detection methods compared to the previous algorithm, the way of dealing with the edge pixels is also modified. The edge pixels are no longer all assigned as a single segment among the $S$ segments in the segmentation map. In fact, they are not considered to belong to any of the $S$ segments in the segmentation map.

### *Adaptive bilateral filtering in L*a*b**

Different images can have different levels of noise. The purpose of applying bilateral filtering [5] is to smooth the relatively smooth areas and save the sharpness of the large-scale edges of the image without blurring. But the parameters of the bilateral filter need to be manually adjusted according to the bilateral filtering results for each image to reach the purpose stated above. Otherwise, either the noise cannot be removed as desired so that the edge detector detects edges along with noisy pixels or the sharpness of edges is weakened. In this case, the parameters of the bilateral filter should be determined separately for each image.

The expression of the bilateral filter with the CIE $L^*a^*b^*$ color space model [8] [9] is shown below.

$$BF\{I_k[m_0,n_0]\} = \frac{1}{N}\sum_{m=m_0-W}^{m_0+W}\sum_{n=n_0-W}^{n_0+W} exp\left(-\frac{(m-m_0)^2+(n-n_0)^2}{2\sigma_d^2} - \frac{\Delta E^2(I_k[m,n],I_k[m_0,n_0])}{2\sigma_r^2}\right) I_k[m,n], \quad \text{where } k \in L^*,a^*,b^* \text{ for the } k \text{ of } I_k \tag{1}$$

$I_k$ is the $k$-th channel of the image, $\sigma_d$ is the standard deviation of spatial smoothing, and $\sigma_r$ controls the range of color difference. The $\sigma_d$ is fixed by the image size: $\sigma_d = 2\%$ of the diagonal of the image. Out determination of the $\sigma_r$ uses the cluster map generated by the K-means method.

The output of the K-means clustering result, the cluster map, is an image with index values from 1 to $K$ representing the cluster label to which each pixel is assigned. For each cluster label, the pixels with the same cluster label are grouped. For each pixel $[m_0,n_0]$ in the $k$-th cluster, the ratio $R_{k,[m_0,n_0]}$ between the range domain value $V_{range}$ and the spatial domain value $V_{spatial}$ is calculated as shown below.

$$V_{range}[m,n;m_0,n_0] = \Delta E^2(I_k[m,n],I_k[m_0,n_0]) \tag{2}$$

$$V_{spatial}[m,n;m_0,n_0] = (m-m_0)^2+(n-n_0)^2 \tag{3}$$

$$R_{k,[m,n;m_0,n_0]} = V_{range}[m,n;m_0,n_0]/V_{spatial}[m,n;m_0,n_0] \tag{4}$$

Next, we average the ratio factor over the $W \times W$ window centered at $[m_0,n_0]$ to obtain $R_{k,[m_0,n_0]}$.

$$R_{k,[m_0,n_0]} = \frac{1}{N}\sum_{m=m_0-W}^{m_0+W}\sum_{n=n_0-W}^{n_0+W}(R_{k,[m,n;m_0,n_0]}) \tag{5}$$

Finally, we average $R_{k,[m_0,n_0]}$ over all the pixels in the $k$-th cluster to obtain the overall ratio factor $R_k$.

$$R_k = \frac{1}{|\Omega_k|}\sum_{[m_0,n_0]\in\Omega_k} R_{k,[m_0,n_0]} \tag{6}$$

Here $\Omega_k$ denotes the set of pixels in the $k$-th cluster. Then, the $\sigma_r$ for cluster label $k$ can be calculated as follows:

$$\sigma_{r,k} = \sigma_d \cdot \sqrt{f \cdot R_k} \tag{7}$$

$f$ here can be assigned any reasonable value that is larger than 1, since over the smooth area, the range domain value must be dominated by the spatial domain value. Here $f = 2$ is applied. With this algorithm, the value of $\sigma_r$ is adaptive according to each cluster within the image.

***Figure 4.*** *Adaptive Bilateral Filtering [5] with color-cluster-dependent selection of $\sigma_r$: original image (left), adaptive bilateral filtering with fixed $\sigma_r$ (center), adaptive bilateral filtering with color-cluster-dependent selection of $\sigma_r$ (right).*

As shown in the Fig. 4, this adaptive bilateral filtering with cluster-dependent $\sigma_r$ removes clutter, while preserving important edges. It approximates a Gaussian filter in the relatively smooth areas while saving the large-scale edges without manual inspection and adjustment of the parameters.

### *Color-aware Sobel edge detector*

The way of applying the Sobel edge detector to a single channel image is trivial [10]. However, the way of combining the Sobel edge detection results on multi-channel images is debatable. Let the Sobel edge detection results applied to each

channel of the $L^*a^*b^*$ space [8] [9] image be denoted as

$$\begin{bmatrix} |g_k| \\ \theta_k \end{bmatrix} = \begin{bmatrix} \sqrt{g_H^2[m,n] + g_V^2[m,n]} \\ \arctan\left(\frac{g_V[m,n]}{g_H[m,n]}\right) \end{bmatrix} \tag{8}$$

where $g_V$ is the result after applying vertical derivative filter and $g_H$ is the results after applying horizontal derivative filter, $|g_k|$ is the gradient magnitude, which is the vector summation of the vertical and horizontal gradient values, and $\theta_k$ is the gradient direction, $k \in L^*, a^*, b^*$. Jumabayeva [1] mentions a method for calculating the combined color gradient magnitude $|g|$ as

$$|g| = \sqrt{\sum_{k \in L^*a^*b^*} |g_k|^2} \tag{9}$$

However, this method cannot distinguish between situations where the gradient magnitude changes are largely due to changes in lightness and situations where the gradient magnitude changes are largely due to changes in chroma. If a real edge lies between these two situations, the edge will not be detected as desired. To address this concern, inspired by the color science concepts summarized by Gevers [6], our color-aware Sobel edge detection method is proposed as follows.

As described above, after the Sobel edge detector is applied to each channel of the $L^*a^*b^*$ space image separately, the resulting gradient magnitude and gradient direction are $\begin{bmatrix} |g_k| \\ \theta_k \end{bmatrix}$, $k \in L^*, a^*, b^*$. Then, the gradient magnitude $|g_L|$ for the $L$ channel stays the same, and $|g_C|$ for the chroma channel is obtained as

$$\begin{aligned} g_C &= |g_a| \angle \theta_a + |g_b| \angle \theta_b \text{ in polar coordinate system} \\ |g_C| &= \sqrt{(|g_a| \cos\theta_a + |g_b| \cos\theta_b)^2 + (|g_a| \sin\theta_a + |g_b| \sin\theta_b)^2} \end{aligned} \tag{10}$$

$|g_L|$ captures the gradient magnitude reflecting lightness, while $|g_C|$ captures the gradient magnitude reflecting colors. The edge map is the union of the thresholded gradient magnitude for the $L$ channel ($|g_L|$) and the thresholded gradient magnitude for the chroma channel ($|g_C|$) as below. The thresholds are chosen according to the thresholding method in the Canny operator [11].

$$\text{EdgeMap} = thr(|g_L|) \cup thr(|g_C|) \tag{11}$$

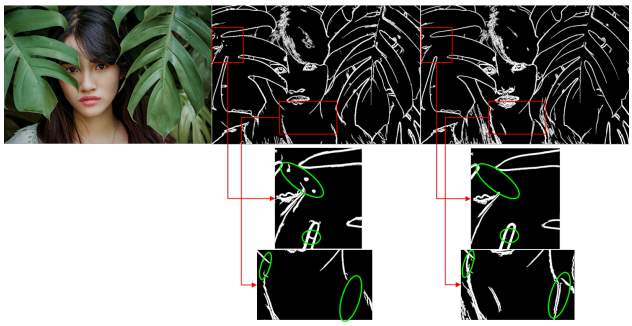

***Figure 5.*** *Color-aware Sobel edge detection. Original image (left), Sobel detection result based on Jumabayeva's method [1] (center), Color-aware Sobel edge detection result (right).*

As shown in the Fig. 5, the Color-aware Sobel edge detector preserves more continuous edges in some color transition areas and at same time removes some isolated features compared to Jumabayeva's method. It is more sensitive to subtle color changes.

### *Generate the merged map from the segmentation map and cluster map*

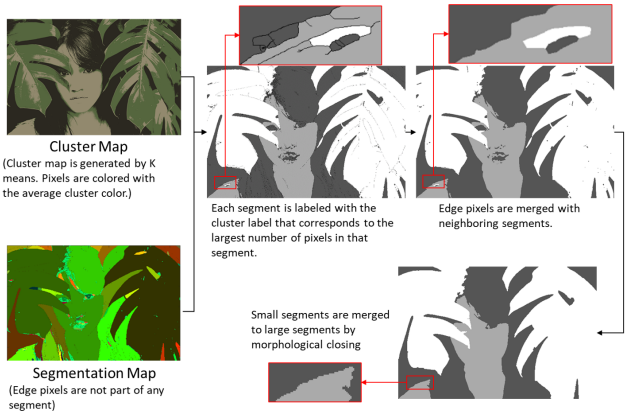


***Figure 6.*** *The process for generating the merged map.*

The merged map is produced with the segmentation map and the cluster map generated by the K-means clustering method. As shown in Fig. 6, each segment in the segmentation map is labeled with the cluster label $k$ that corresponds to the largest number of pixels in that segment. Each edge pixel, which is not initially considered to belong to any of the $S$ segments, is individually assigned to cluster $k$ if there is a single cluster number $k$ that occurs the maximum number of times among the neighbors of that edge pixel. If no single cluster number $k$ satisfies this condition, then the range of neighbor pixels are enlarged until finding the single cluster number $k$, or the range has been enlarged three times. If the neighbor range has been enlarged three times, then the pixel will be assigned to the cluster with the smallest cluster number among the cluster number candidates. The merged map is finalized by merging the small segments to large segments according to the following process: the image is down-sampled by $8\times$, then processed with a cross shape structuring element of size $3 \times 3$ by morphological closing, and up-sampled back by $8\times$. The small clutters are removed by this procedure, which prevents meaninglessly frequent switches to the screen assignments.

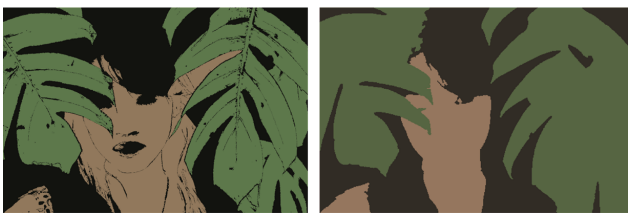

***Figure 7.*** *Merged map result comparison: Jumbayeva's method[1] (left) and new method (right). Each cluster is displayed with the mean color for that cluster.*

As shown in the Fig. 7, compared to Jumabayeva's method [1], several improvements stand out. Edge pixels are merged to

neighboring segments. The parameters for bilateral filtering are not manually selected, and no small segments appear.

### *Selection of the best screen assignments while further merging clusters*

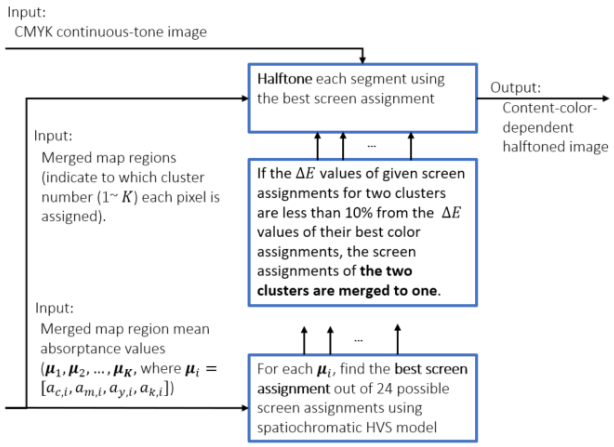


***Figure 8.*** *Selection of the best screen assignments while merging clusters.*

This step finds the best screen assignment for each cluster and halftones each segment with its best screen assignment. The flow chart is shown in Fig. 8. The pixels in the merged map are indexed with cluster numbers from 1 to $K$. The mean absorptance values $((\mu_1, \mu_2, \cdots, \mu_K)$, where $\mu_i = [a_{c,i}, a_{m,i}, a_{y,i}, a_{k,i}])$ for the $K$ clusters in CMYK color space are calculated based on both the merged map and the CMYK continuous-tone image. For each mean abosorptance value $\mu_i$, the best screen assignment out of 24 possible screen assignments using the spatiochromatic HVS model is selected.

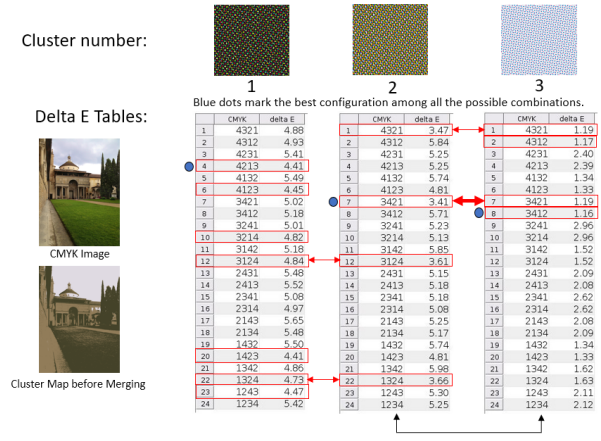


***Figure 9.*** *Process of merging the screen assignments of two clusters. The blue dots indicate the best screen assignment for the cluster. The red boxes cropped the screen assignments with $\Delta E$ values less than 10% from their own best screen assignments.The red arrows mark the candidate screen pairs for merging. The bold red arrow marks the final merged screen assignment for cluster number 2 and cluster number 3.*

Compared to Jumabayeva's method, the novel part of the algorithm lies in the following operations. For each cluster, the $\Delta E$ values ($\Delta E$, with size of $24 \times C$, where 24 is the total number of screen assignments and $C$ is the total number of clusters) are calculated between the halftone color patches generated by all possible screen assignments and the continuous-tone color patch with mean absorptance value corresponding to that cluster. The screen assignments of the two clusters are merged to one if the $\Delta E$ values of a given screen assignment for two clusters are less than 10% from their own best screen assignment's $\Delta E$ values ($\Delta E_{opt}$ with size of $1 \times C$). If there are multiple choices for a cluster to merge, among all the screen assignment pair candidates ($[i,[A,B]]$, where $i$ indicates the screen assignment index, $A$ and $B$ are the cluster numbers), only the the pair with smallest sum of percentage differences from their best screen assignments will be chosen to be merged as shown in Fig. 9 and the algorithm below. That is to say, the regions of different cluster indices may use the same screen assignment. This reduces the number of clusters used in the halftoning process and avoids frequent switches between screen assignments.

**Algorithm 1:** Merging Clusters Algorithm

**Result:** The merged clusters
Initial $\Delta E_{1-hot} = \Delta E < 1.1 \cdot \Delta E_{opt}$ ;
Initial $\Delta E_{percent} = \Delta E / \Delta E_{opt}$ ;
Initialize a graph structure with $C$ vertices;
**for** *cluster A* **do**
  **for** *screen assignment pair candidates* $[i,[A,B]]$ **do**
    Calculate $S_i = \Delta E_{percent}[i,A] + \Delta E_{percent}[i,B]$;
  **end**
  Find the smallest $S_i$ value and assign it to be the edge value from vertex $A$ to vertex $B$;
**end**
**if** *vertex A has more than* 1 *edge* **then**
  Assign the edge with the smallest edge value to be the only edge connected to vertex $A$;
**end**
Remaining edges are the connecting the pairs of the merged clusters.;

With the best screen assigments, each region is halftoned. And this is the content-color-dependent halftoned image result.

## Experimental Results

The CCDS halftoned result and the 180% enlargement of a screen transitions area are shown in the Fig. 10. The resulting CCDS halftone image has no texture discontinuity when switching screens either between the flesh tone area and black background area or between black background area and the green leaves area.

The comparison between the 180% enlargement of the halftoned image using the single best screen assignment according to the whole image and the zoom-in of our updated CCDS method is shown in Fig. 11. It is easy to find that the zoom-in in transition area of the CCDS halftoned image is less noisy for all the color regions, except the small green leaf.

A comparison between the enlargement of a halftoned image using CCDS without edge detection method and the updated CCDS method is shown in Fig. 12. Clearly, contouring artifacts can occur if the screen assignment is switched within a smooth re-

***Figure 10.*** *The original image (left of the first row), the segmentation map (second row), and 180% enlargement of the CCDS halftone results (right of the first row). The red boxes mark the enlarged region.The reader is advised to zoom in on the enlargement by a sufficient amount to eliminate any display artifacts due to subsampling of the enlarged halftone image.*

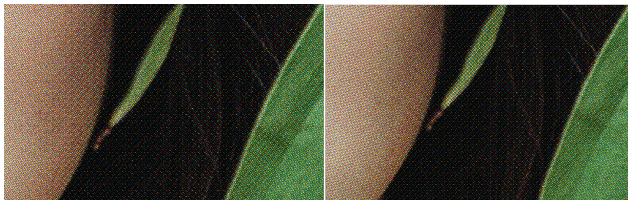

***Figure 11.*** *The 180% enlargements of a portion of the halftone image. The halftone image with a single screen assignment (left). That screen assignment is selected with the smallest $\Delta E$ value calculated based on the whole image. The halftone image with the improved CCDS algorithm (right). The reader is advised to zoom in on the enlargements by a sufficient amount to eliminate any display artifacts due to subsampling of the enlarged halftone images.*

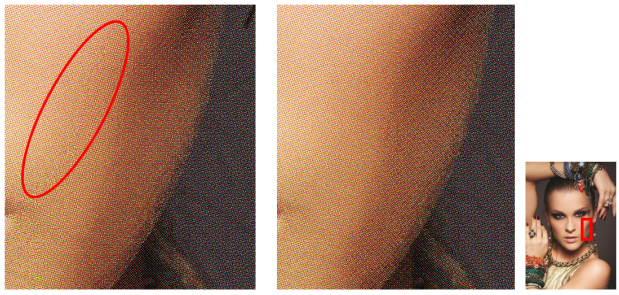

***Figure 12.*** *The left two images are enlargements of a portion of the halftone image shown on the right. The leftmost halftone image is generated by CCDS without the edge detection method. The middle image is generated by our improved CCDS method. The red oval crops the area where the screen switch is accompanied by a contouring artifact. The reader is advised to zoom in on the enlargements by a sufficient amount to eliminate any display artifacts due to subsampling of the enlarged halftone images.*

gion of the image. Our color-aware Sobel edge detector prevents this from occurring by restricting screen assignment switches to only occur across edges in the image.

## Conclusion

The updated CCDS algorithm inherits from Jumabayeva's method and refines the details of the implementation. It makes the number of clusters be determined by an algorithm instead of being manually selected by the user. An adaptive bilateral filter is developed as a general noise-removal pre-process before doing edge detection. So, the images with different noise levels are treated with the bilateral filter adaptive to their specific noise levels. The color-aware Sobel edge detection is more sensitive to subtle color changes than the previous method, so the segmentation map becomes clearer and more reasonable. Also, the updated CCDS algorithm applies several steps for the purpose of preventing frequent switches between screens in the final halftoned image; so most of the screen switches are necessary switches to achieve the best quality.

## References


[1] A. Jumabayeva, et al., Content-color-dependent screening (CCDS) using regular or irregular clustered-dot halftones, 2018 7th European Workshop on Visual Information (EUVIP). IEEE. (2018).

[2] H. R. Kang, Digital color halftoning. SPIE press, 1999.

[3] F. A. Baqai, and J. P. Allebach, Computer-aided design of clustered-dot color screens based on a human visual system model, Proceedings of the IEEE. 90, pg. 104-122. (2002).

[4] Y. Chen, et al., The lattice-based screen set: a square n - color all-orders moiré-free screen set, IEEE Transactions on Image Processing, 25, pg. 1873 – 1886. (2016).

[5] B. Zhang and J. P. Allebach, Adaptive Bilateral Filter for Sharpness Enhancement and Noise Removal, IEEE Transactions on Image Processing, 17, pg. 664-678. (2008).

[6] T. Gevers, et al., Color in computer vision: fundamentals and applications. John Wiley & Sons, 2012, pg 43.

[7] M. A. Syakur, et al., Integration K-Means Clustering Method and Elbow Method For Identification of The Best Customer Profile Cluster., IOP Conference Series. Materials Science and Engineering, 336, 1 (2018).

[8] K. McLaren, The development of the CIE 1976 (L*a*b*) uniform colour space and colour-difference formula, Journal of the Society of Dyers and Colourists, 92, 9, Blackwell Publishing Ltd, pg. 338-341. (1976).

[9] S. Hu, Z. Pizlo, and J. P. Allebach, JPEG ringing artifact visibility evaluation, Image Quality and System Performance XI, 9016, Part of SPIE IS&T Electronic Imaging, (2014).

[10] P. E. Danielsson and O. Seger, Generalized and separable Sobel operators, Machine Vision for Three-Dimensional Scenes, Academic Press, FL, pg. 347 – 381. (1990).

[11] J. Canny, A computational approach to edge detection, IEEE Transactions on Pattern Analysis and Machine Intelligence, 8, pg. 679–698. (1986).

[12] T. Zhang and C. Y. Suen, A fast parallel algorithm for thinning digital patterns, Communications of the ACM, 27, pg. 236–239. (1984).

[13] K. Benhamza and H. Seridi, Canny edge detector improvement using an intelligent ants routing, Evolving Systems, pg. 1-10. (2019).

[14] Y. F. Liu, et al., Multi-mode Halftoning Using Stochastic Clustered-Dot Screen, Frontier Computing (464), pg 423-31. (2018).

[15] Y. F. Liu and J. M. Guo, Clustered-dot screen design for digital multitoning, IEEE Transaction and Image Process, 25(7), pg 2971–2982. (2016).

## Author Biography

*Yang Yan received her B.S. (2016) Electrical Engineering from Purdue University and currently is a Ph.D. student from Purdue ECE department. Her primary area of research has been image processing, image quality evaluation, and machine learning.*

*Jan P. Allebach is Hewlett-Packard Distinguished Professor of Electrical and Computer Engineering at Purdue University. Allebach was named Electronic Imaging Scientist of the Year by IS&T and SPIE, and was named Honorary Member of IS&T, the highest award that IS&T bestows. He has received the IEEE Daniel E. Noble Award, the IS&T/OSA Edwin Land Medal, the IS&T Johann Gutenberg Prize, is a Fellow of the National Academy of Inventors, and is a member of the National Academy of Engineering.*

# JOIN US AT THE NEXT EI!

IS&T International Symposium on

# Electronic Imaging

SCIENCE AND TECHNOLOGY

*Imaging across applications . . . Where industry and academia meet!*

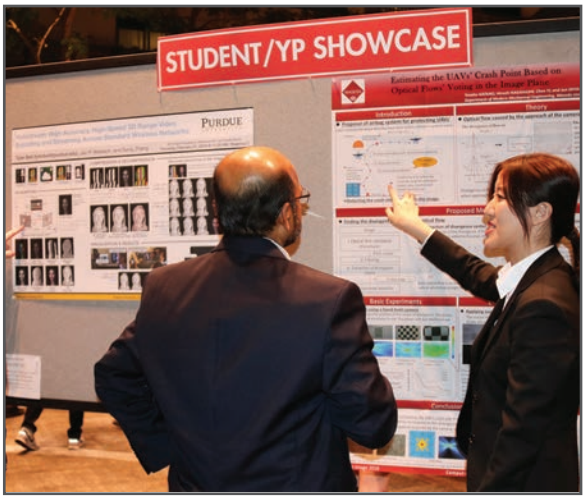


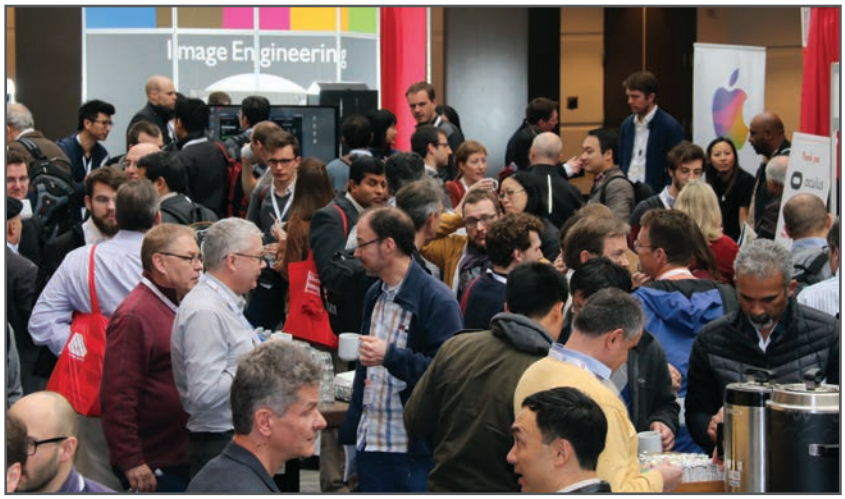



**• SHORT COURSES • EXHIBITS • DEMONSTRATION SESSION • PLENARY TALKS •**
**• INTERACTIVE PAPER SESSION • SPECIAL EVENTS • TECHNICAL SESSIONS •**

**www.electronicimaging.org**

IS&T
imaging.org